I&EC research
Industrial & Engineering Chemistry Research

pubs.acs.org/IECR

Article

Ionic Liquid Welding of the UIO-66-NH_2 MOF to Cotton Textiles

Meagan A. Bunge, Erick Pasciak, Jonglak Choi, Luke Haverhals, W. Matthew Reichert, and T. Grant Glover*

Cite This: *Ind. Eng. Chem. Res.* 2020, 59, 19285−19298

Read Online

ACCESS | Metrics & More | Article Recommendations | Supporting Information

ABSTRACT: Ionic liquid based fiber welding has been used to attach the metal−organic framework (MOF) UiO-66-NH_2 to cotton fibers. The results show that by controlling the extent of the welding process, it is possible to produce fibers that contain a high surface area (approximately 50−100 m^2/g), an X-ray diffraction pattern consistent with UiO-66-NH_2, and fibers that are chemically reactive to dimethyl 4-nitrophenyl phosphate (DMNP), a common chemical weapon simulant. The ionic liquid/MOF welding solution can be applied by directly placing the fabric in the welding solution or by utilizing an airbrushing technique. Both welding techniques are shown to be scalable with results collected on approximately 1 × 1, 5 × 5, and 15.5 × 15.5 in. swatches. The results are also applicable to weaving methods where the MOF is welded to individual threads and subsequently woven into a textile. The results provide an industrially scalable method of attaching a wide variety of MOFs to cotton textiles, which does not require synthesizing the MOF in the presence of the textile.

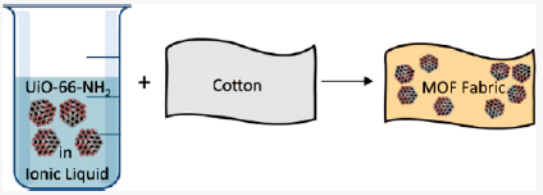

INTRODUCTION

Metal−organic framework (MOF) fibers have been produced using a variety of different methods including electrospinning, atomic layer deposition (ALD), and other approaches.[1−10] In many cases, these methods were applied to synthetic polymers with only limited work completed on cotton fibers. Regarding cotton fibers, the work of Hinestroza showed that it is possible to grow MOFs using a carboxymethylation method,[5] and the Glover group has shown that it is possible to grow Cu-BTC and UiO-66-NH_2 MOFs on fibers using a reactive dye method (RDM).[1,2] However, it would be helpful to have a process capable of attaching a broad range of different adsorbent materials, such as MOFs, covalent organic frameworks (COFs), polyoxometalates (POMs), or other adsorbents, without having to synthesize the adsorbent in the presence of the fibers. Decoupling the adsorbent synthesis from the fiber attachment may allow the use of known adsorbent synthesis steps and avoid having to invent customized adsorbent synthesis routines that are amenable to fiber stability.

One approach to this problem is to utilize ionic liquid (IL)-based solvent welding of adsorbents to cellulose fibers. ILs are broadly comprised of cation−anion pairs, where the large covalently bonded molecular structure of these cations and anions is significantly different from common naturally occurring ionic compounds, such as sodium chloride. Regarding sodium chloride, the sodium cation and chloride anion are essentially spherical ions containing an evenly distributed positive and negative charge, respectively. The net attraction between these two ions creates areas of partial charge density around the spherical atoms. With the association of similar ionic pairs, these partial charges create a three-dimensional crystal lattice structure. Although these ionic compounds can often be easily dissociated using polar solvents such as water, the strong ionic bonds of the pure ionic substances and close packing of the ions create relatively high melting points, such as the 801 °C melting point temperature for sodium chloride.[11,12]

However, the structures of IL cations are commonly comprised of an asymmetric organic molecule with a positive charge centered on a nitrogen or phosphorus molecule with various organic side chains.[13,14] The *n*-alkyl chain length of the IL cations plays a significant role in the melting points, viscosity, and liquid range of these compounds. Although the monatomic halogen atoms of Cl^-, Br^-, or I^- are commonly used as anions, especially during synthesis, weakly basic organic or inorganic polyatomic compounds with a protected negative charge are often seen in room-temperature ILs.[15,16]

It has been shown in the literature that simple ILs can be used to dissolve cellulose. This concept has been applied to develop the process known as natural fiber welding where an IL partially dissolves the cellulose allowing for a manipulation of the cellulose properties.[17] Specifically, upon application, the IL swells the cellulose as it disrupts the intermolecular hydrogen bonding of the fibers. During this time, mobilized material from neighboring fibers intermingles and forms an entangled structure that, upon removal of the IL via a water wash, become fixed in an entangled state. It has been

Received: July 29, 2020
Revised: September 28, 2020
Accepted: September 28, 2020
Published: September 28, 2020

https://dx.doi.org/10.1021/acs.iecr.0c03763
Ind. Eng. Chem. Res. 2020, 59, 19285−19298

previously shown that IL-welded cloth that includes a water wash step shows a negligible change in sample mass as a result of the treatment process, which indicates that the IL is not retained in the material.[17] The extent that the fibers are altered depends on a variety of experimental parameters such as the type of fibers, the type of IL used, the exposure time, and the extent of any heating steps.[18] Moreover, during the dissolution, additives can be encapsulated into the partially dissolved fibers to produce a functionalized material.[17−19]

The initial work in this area has shown that by welding the loose natural fibers of the textile, a stronger textile results and that control over the properties of the textile can be adjusted by the amount of IL used to complete the welding.[17−22] Trulove et al. demonstrated the ability to utilize the mobility of the individual fibers to encapsulate a variety of nanomaterials within a biopolymer matrix using this technique.[19] They showed that a catalyst could be encapsulated in a linen yarn by first coating the yarn with a catalyst ink formed from a suspension of the catalyst in the IL. The yarn was then coated with the ink, and after a welding period, the IL was removed. The resulting yarn consisted of catalyst impregnated into the yarn structure by a sheath of biopolymer. The impregnated yarn was tested for catalytic activity and showed that the catalyst was still active after the process.

However, when considering welding fibers to contain porous structures, it is reasonable to assume that ILs could enter the pores of almost any porous structure. Glover et al. examined this concept and impregnated ILs in porous silica and activated carbon and examined the composites as possible sorbents for CO_2 capture.[23,24] The authors found that for a 40 Å pore MCM-41, none of the studied ILs were able to be loaded into the pores. However, the same ILs were readily impregnated into the pores of a 90 Å SBA-15 and when washed with a solvent, the IL could be removed from the pores. When impregnating activated carbon (Calgon Carbon Corp. BPL type carbon[25]), it appeared that the macro- and mesopores were filled by the IL, but the micropores were not filled because of space limitations.[23]

With these results in mind, the purpose of this work is to show that MOFs can be attached to cotton textiles using IL-welding techniques and that the MOF will maintain its high surface area and reactive nature after being attached to the fiber. A wide variety of MOFs could be selected for this purpose, but for this work, UiO-66-NH_2 has been selected because this material has been the subject of other MOF fabric studies and because UiO-66-NH_2 has a window size less than 6 Å, which is not likely to allow ILs to enter the pore structure.[1−4,6−9,26]

■ EXPERIMENTAL SECTION

UiO-66-NH_2 and $Zr(OH)_4$ powders were provided by the Combat Capabilities Development Command (CCDC) Chemical Biological Center (CBC) U.S. Army Futures Command and used as received. Synthesis methods for these materials are available elsewhere.[2,10] Several different sizes of cotton textiles were functionalized using ILs, and different application procedures were examined as detailed below.

Direct-Contact Method. A welding solution was prepared by mixing the IL, 1-ethyl-3-methylimidazolium acetate (EMIm OAc), and the MOF, UiO-66-NH_2. The welding solution contained 100−200 mg of UiO-66-NH_2 and 0.5−2 g of the IL depending on the sample. The IL was purchased from MilliporeSigma and used as received. The IL was not diluted with a solvent. The welding solution was directly applied to an approximately 1 × 1 in. swatch of cotton and pulled across the swatch using a doctor blade. Prior to preparing the fabric, an aluminum block was placed in an oven that was preheated to 80 °C. After preparing the fabric, it was placed on the aluminum block in the oven and then a second block of aluminum was placed on top of the fabric. Once the fabric sample was removed from the oven, it was washed in water for 24 h in a beaker under agitation to remove the IL as well as any loose MOF. This same process was also used for 5 × 5 and 15.5 × 15.5 in. swatches. For the 5 × 5 in. swatch, 2.5 g of UiO-66-NH_2 was placed in 6 g of the IL and for the 15.5 × 15.5 in. swatch, 26 g of UiO-66-NH_2 was placed in 127.5 g of the IL. Swatch dimensions mentioned above are based on the fabric swatch prior to modification and some shrinking did occur as discussed below.

The names of the samples follow the convention: [the mass of MOF used, the number of sides of the fabric the MOF/IL was applied to, the time the sample stayed in the oven, and the amount of IL used]. For example, [100 mg, 2 sides, 5 h, and 0.7 g IL] indicates that 100 mg of MOF was placed into the IL, the solution was applied to both sides of the fabric, the reaction was allowed to run for 5 h, and 0.7 g of the IL was used.

Airbrush Method. In addition to producing fabric samples with the direct-contact method, samples were also prepared using an airbrush. The IL/UiO-66-NH_2 mixture was added to the airbrush and sprayed onto the fibers. Then, the swatch was placed in an oven at 80 °C, subsequently removed from the oven, and washed following the same procedure as the direct-contact method samples. Three 2 × 2 in. airbrush samples were prepared. The sample designated Airbrush 1 was prepared using 2.5 g of the IL and 0.3 g of the MOF (following the naming convention mentioned above, the sample was referred to as [Airbrush 1 0.3 g, 2 sides, 2 h, 2.5 g IL]), Airbrush 2 was prepared with 2.1 g of the IL and 0.4 g of the MOF, and Airbrush 3 was produced using 4.1 g of the IL and 0.75 g of the MOF (designated [Airbrush 2 0.4 g, 2 sides, 2 h, 2.1 g IL] and [Airbrush 3 0.75 g, 2 sides, 2 h, 4.1 g IL], respectively). For the 15 × 16 in. large airbrush sample, the welding solution contained 35 g of UiO-66-NH_2 in 241.7 g of the IL. However, when applying the solution using the airbrush, the fabric was sprayed until the point of wetness such that the fabric did not appear to absorb any more welding solution, and in many cases, this did not result in the utilization of all the IL/MOF welding solution that was prepared.

Yarn Method for Woven Fabrics. Fabrics were also developed by first welding UiO-66-NH_2 onto yarns which were then woven into fabrics of various sizes. The process began with a 13 single (normal English) ring-spun cotton yarn that was pulled through a solution of EMIm OAc, dimethyl sulfoxide (DMSO), and dissolved cellulose nanocrystals (CNCs) and a suspension of UiO-66-NH_2. Then, the coated yarn was passed through an 80 °C heat exchanger and into a room-temperature water bath to remove the cosolvents. As discussed below, one sample was also prepared using a 70 °C welding temperature. The resulting yarns were dried in a 60 °C oven and then woven using commercially purchased hand looms (Clover Mini Weaving Loom or Schacht Cricket Loom).

Control Experiments. *Stability of the MOF in the IL.* Two samples were prepared to evaluate MOF stability in the IL, and each sample was prepared by adding 200 mg of UiO-66-NH_2 and 1 g of EMIm OAc into a 20 mL vial, which was

https://dx.doi.org/10.1021/acs.iecr.0c03763
Ind. Eng. Chem. Res. 2020, 59, 19285−19298

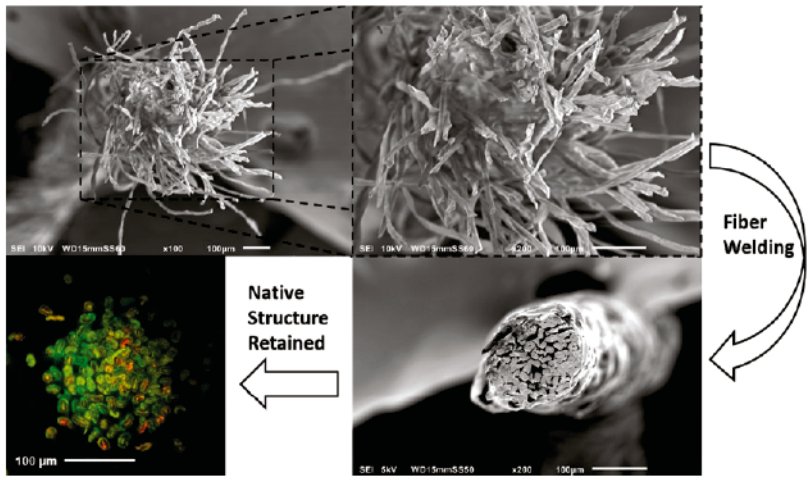

Figure 1. Examples of fiber-welding cotton yarn. The topmost images are scanning electron microscopy images of a yarn cross section prior to fiber welding. Fibers are easily separated as they are only held together by friction. The lower images are of "welded" cotton yarn cross sections after controlled processing. Yarns are consolidated into a tight bundle because hydrogen bonding (intermolecular forces) has been extended between neighboring cotton fibers. The confocal fluorescence lifetime imaging at the lower left shows that the native order and structure has been retained—for example, the lumens of individual fibers can be resolved by the fluorescence lifetime data (orange-colored line structures at the center of many of the cotton fibers).

then stirred. Both vials were placed in the oven at 80 °C, but one vial was removed from the oven after 2 h and the other after 5 h. After the sample was removed from the oven, the mixture was placed in a beaker with water and stirred for 24 h. During that time, the water was replaced three times with fresh water. This was done by stopping the stirring, allowing the MOF to settle to the bottom of the vial, and pipetting off the water and replacing it. Once the new water was added to the MOF, the stirring resumed. At the end of 24 h, the MOF and water mixture was filtered, and the MOF particles were collected for analysis.

Cotton Welded with IL Only. Control Sample #1. Using a glass stir rod, 6 g of EMIm OAc was applied to both sides of a 4.5 × 3.5 in. swatch. The sample was kept in the oven for 2 h at 80 °C. Once removed from the oven, the sample was placed in a beaker with water and stirred for 24 h while periodically changing the water.

Control Sample #2. Using a glass stir rod, 1 g of EMIm OAc was applied to both sides of a 1 × 1 in. swatch. The sample was kept in the oven for 2 h at 80 °C. Once removed from the oven, the sample was placed in a beaker with water and stirred for 24 h while periodically changing the water.

Control Sample #3. A 1.5 × 1.5 in. swatch was dipped in 1 g of EMIm OAc and then a doctor blade was used to spread the IL across the fabric. Before the fabric was placed in the oven, the swatch was pressed between paper towels to remove any excess IL. After baking in the oven at 80 °C for 2 h, the sample was placed in a beaker with water and stirred for 24 h while periodically changing the water.

Analysis and Characterization. Nitrogen adsorption isotherms were measured using a Micromeritics 3 Flex or 2020 porosimeter, and this data was used to calculate the BET surface area using the Rouquerol criteria.[27] Powder X-ray diffraction (PXRD) analysis was completed using a PROTO AXRD and care was taken to load the fabric such that a flat surface was available for diffraction. Dimethyl 4-nitrophenyl phosphate (DMNP) reaction rate data were collected as has been detailed elsewhere using a Thermo UV/VIS instrument.[2] Scanning electron microscopy (SEM) measurements were completed using an FEI Quanta 250 scanning electron microscope instrument, and gold sputtering was completed on each sample. For the data shown in Figure 1, a JEOL JSM-6010Plus/LA scanning electron microscope was utilized, and the samples were sputtered with gold using a Crossington 108 Auto/SE sputter coater along with an MTM-20 high-resolution thickness controller. The specimens were cut using a scalpel and supported on aluminum stubs with carbon tape. To collect the fluorescence image, the sample yarn was dyed with Rhodamine B in the aqueous solution and dried in air, and a Becker & Hickl time-correlated single photon-counting fluorescence lifetime-imaging microscope was utilized to collect the image. Thermal gravimetric analysis was performed using a NETZSCH TG 209 F1, and samples were heated using a ramp rate of 5 °C/min to 800 °C while under an air flow. The weight percent of the MOF in the fabric was calculated using the method of Lu, where the mass of the MOF in the fabric is determined based on the ratio of the weights at 300 °C to that of 750 °C of pure UiO-66-NH_2. We have assumed that all the IL has been removed during the washing step and that any organic residue at 750 °C is negligible.[8]

■ RESULTS AND DISCUSSION

The changes that take place to cotton fibers after exposure to a welding solution have been detailed elsewhere and a summary picture is shown in Figure 1.[17] As shown in the figure, the individual fibers within cotton yarns are greatly consolidated after exposure to the IL welding solvent. Even so, the fluorescence imaging data clearly show that the native structure is retained (e.g., the lumens of individual fibers are still visible). This is possible because the IL partially dissolves just the outermost cellulose at the exterior of individual fibers, and when the IL is removed from the fibers using a washing solvent, the cellulose from adjacent fibers is able to interact through an extended hydrogen-bonding (intermolecular) network.

Direct-Contact Welding Process. In the first method, UiO-66-NH_2 was placed in 1-ethyl-3-methylimidazolium

https://dx.doi.org/10.1021/acs.iecr.0c03763
Ind. Eng. Chem. Res. 2020, 59, 19285−19298

acetate (EMIm OAc) (Figure 2) and mixed to suspend the MOF particles in the IL. The IL/MOF solution was then

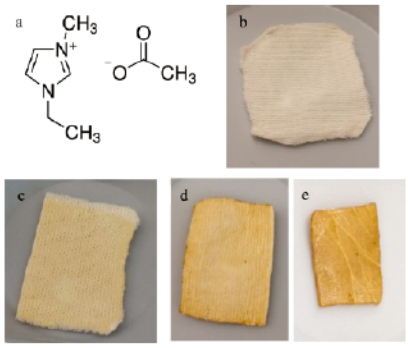

Figure 2. (a) Structure of the IL 1-ethyl-3-methylimidazolium acetate used to weld cotton fibers with UiO-66-NH_2 MOF, (b) plain cotton swatch compared to (c–e) fabric swatches that have been modified with UiO-66-NH_2 and via the IL welding process. (c) [100 mg, 1 side, 5 h, 0.3 g IL], (d) [100 mg, 2 sides, 5 h, 0.7 g IL], and (e) [200 mg, 2 sides, 5 h, 2 g IL]. Samples are approximately 1–1.5 $in.^2$ in size.

placed directly onto an approximately 1 × 1 in. fabric swatch and the fabric, heated, and washed as described in the Experimental Section. The naming convention for these samples is provided in the Experimental Section, and the swatches are shown in Figure 2. Compared to the cotton control fabric shown in Figure 2b, all of the MOF IL-welded fabrics have a color consistent with UiO-66-NH_2 powder with the yellow color increasing with more MOF contained in the IL solution or when both sides of the fabric are welded. The sample shown in Figure 2e was unique amongst the samples because this sample was welded to the extent that the textile was more similar to rigid plastic. Because the MOF is applied as a suspension, the application of the welding solvent can be limited to one side or the other of the fabric. This is important because it shows that IL welding can be used to provide specific functionalization at specific locations on the fabric.

PXRD patterns of the samples were collected after completing the welding process and are shown in Figure 3. The [100 mg, 1 side, 5 h, 0.3 g IL] sample, shown in Figure 2c, has a PXRD pattern consistent with the pure MOF powder as does the [100 mg, 2 side, 5 h, 0.7 g IL] sample, shown in Figure 2d. The impact of welding time on the PXRD patterns can be seen with the [100 mg, 2 sides, 5 h, 0.7 g IL] sample showing a more defined PXRD pattern than a similar sample allowed to react for only 2 h. However, the [200 mg, 2 side, 5 h, 2 g IL] sample, shown in Figure 2e, does not show an observable PXRD pattern.

The surface areas of the samples are shown in Table 1, where the sample shown with an asterisk indicates that the sample was produced using 100 mg of the MOF in the IL but prepared using new solutions for each side of the fabric. To determine the amount of MOF loaded on each sample, the surface area method of Bunge et al. was used as well as the method of Lu et al. that heats the sample in a thermogravimetric analyzer (TGA).[2,8] The calculations of MOF loading using these two methods are shown in Table 1. The results show that in general, the TGA estimates considerably more MOF present on the fabric than the corresponding calculation via BET surface area. It is possible that the welding process reduces the accessibility of the MOF to nitrogen or that the MOF is damaged during the welding

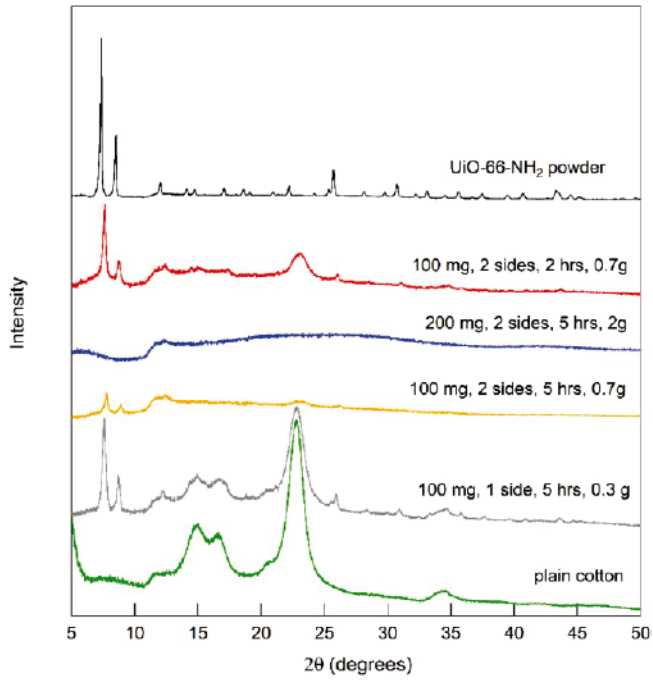

Figure 3. PXRD pattern of samples under various conditions compared to plain cotton and pure UiO-66-NH_2 powder. The MOF powder PXRD pattern has been scaled but all other patterns are shown as measured.

process, which results in a lower surface area and in turn a lower calculated weight percent of the MOF on the fabrics. The TGA method however is not influenced by these situations with the weight percent being calculated based on the degradation of the linker and the mass of the structural building unit in the MOF.[8] As discussed previously, the weight change in fibers after welding and washing with water is effectively unchanged, indicating no residual IL in the fibers, which allows for clear degradation transitions to be identified consistent with MOF thermal degradation.[17] TGA data are provided in the Supporting Information.

The [100 mg, 1 side, 5 h, 0.3 g IL] sample had a surface area of 28 m^2/g compared to 44 m^2/g for the [100 mg, 2 side, 5 h, 0.7 g IL] sample, and the [200 mg, 2 side, 5 h, 2 g IL] sample had 0 m^2/g. The data for the 200 mg sample are interesting as it shows that these welding conditions are impacting the porosity of the MOF. Therefore, to determine the effect of the IL welding conditions on the MOF structure and to determine the impact of the IL welding on the pure textile surface area, control experiments were conducted. First, control experiments were completed by exposing the fabric to the same welding processes that were used to attach the MOF to the fibers, but without the presence of the MOF. Details of these processes are provided in the Experimental Section. In all cases, the control fabrics had no measurable surface area, which indicates that all of the surface area can be attributed to the MOF material. The PXRD patterns of these control samples were also collected, as shown in Figure 4.

Likewise, to evaluate the impact of the IL welding process on the MOF, pure UiO-66-NH_2 powder was exposed to the IL at the same welding conditions but without the presence of fabric. The PXRD results, shown in Figure 5, show that the crystallinity of the MOF is maintained even after exposure to the welding conditions. The pure MOF powder had a surface

https://dx.doi.org/10.1021/acs.iecr.0c03763
Ind. Eng. Chem. Res. 2020, 59, 19285–19298

Table 1. BET and TGA Results

sample	surface area (m^2/g)	% MOF on fabric TGA	% MOF on fabric based on MOF BET	% MOF on fabric based on 2 h IL/MOF control	% MOF on fabric based on 5 h IL/MOF control
[100 mg, 2 sides, 2 h, 0.7 g IL]	89	35	7	12	
[100 mg, 2 sides, 5 h, 0.7 g IL]	44	35	4		15
[100 mg, 1 side, 5 h, 0.3 g IL]	28	12	2		9
[100 mg, 1 side, 5 h, 0.6 g IL]	71	24	6		24
[100 mg, 1 side, 2 h, 0.5 g IL]	58	13	5	8	
[100 mg, 1 side, 5 h, 0.5 g IL]	76	18	6		25
[200 mg, 1 side, 5 h, 1 g IL]	71	18	6		24
[200 mg, 2 sides, 5 h, 2 g IL]	0	40	0		0
[100 mg, 2 sides, 5 h, 0.35 g IL (2nd wash)[a]]	27	14	2		9
[200 mg, 2 sides, 1 h, 0.9 g IL (2nd wash)]	36	15	3	5	
[200 mg, 2 sides, 5.5 h, 0.5 g IL (2nd wash)]	58	15	5		19

[a]Prepared using a new welding solution for each side.

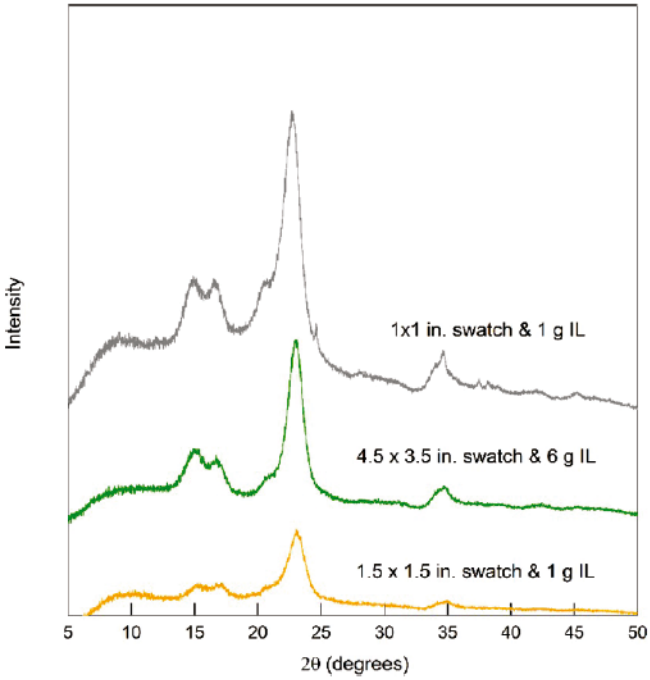

Figure 4. PXRD data for control cotton swatches exposed to the IL welding process without the MOF in the welding solution.

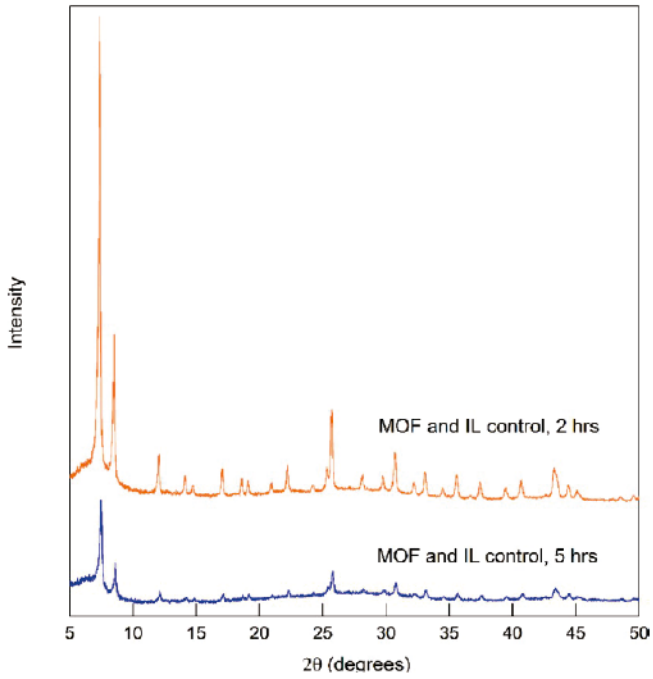

Figure 5. PXRD data for MOF powders exposed to the IL at the same conditions used for the welding but without the presence of fabric.

area of 1255 m^2/g, but when the MOF was in the IL welding solution and the mixture was placed in the oven for 2 h, the surface area was reduced to 758 m^2/g, and when the MOF welding solution was allowed to remain in the oven for 5 h, the surface area was reduced to 301 m^2/g. These results show that prolonged IL welding will reduce the surface area of the MOF but that a large fraction of the porosity is maintained.

This result has implications for how the MOF loading is calculated on the fabric when using the surface area method of Bunge. In particular, the use of the surface area to calculate MOF loading on the fabrics is dependent on the assumption made about the surface area of the MOF on the fibers. Table 1 shows the impact of using the pristine MOF surface area as the basis for MOF fabric loading and the impact of using the surface area of the MOF control powder that was exposed to the IL for 2 and 5 h. In these cases, the fabric-welding time was used to determine which MOF surface area was most appropriate as the basis of the loading calculations. In particular, fabrics welded for 2 h are shown with loadings calculated using the surface area of the 2 h MOF control and likewise for 5 h samples.

The results of the control experiments provide an explanation for the variation of the surface area data and MOF wt % data shown in Table 1. Specifically, when the samples [200 mg, 1 side, 5 h, 1 g IL] and [200 mg, 2 sides, 5 h, 2 g IL] are compared, it is concluded that adding more IL decreased the surface area of the fabric sample to 0 m^2/g. However, the TGA data indicate 40 wt % MOF on the [200 mg, 2 sides, 5 h, 2 g IL] sample. This is consistent with the control data that showed prolonged exposure of the MOF to the IL degrades the MOF. For the two samples being compared here, the time of the welding process was the same, but the amount of IL was changed, which likely resulted in the MOF reacting with the IL such that all the surface area of the MOF was lost. The TGA data are likely reflecting the welding

https://dx.doi.org/10.1021/acs.iecr.0c03763
Ind. Eng. Chem. Res. 2020, 59, 19285−19298

of the Zr structural building unit on the fabric and are not impacted by the loss of the MOF structure.

A similar trend can be observed when comparing the [100 mg, 2 side, 5 h, 0.7 g IL] and [100 mg, 2 side, 2 h, 0.7 g IL] samples, where the PXRD pattern of the sample that was in the welding solution for 2 h is of better quality than the sample that was welded for 5 h. The trends in the PXRD pattern are also consistent with the surface area showing the 2 h welding process that resulted in a higher surface area than the 5 h process. The TGA data show that both samples have 35 wt % MOF, indicating that the MOF has likely degraded, leaving Zr welded on the fibers.

Finally, when comparing the [100 mg, 1 side, 2 h, 0.5 g IL] sample to the [100 mg, 1 side, 5 h, 0.5 g IL] sample, the trends are less obvious. In this case, the sample welded for 5 h produced a higher surface area than the sample welded for 2 h. However, when the TGA data are compared, the data show that the sample welded for 5 h has a higher Zr loading on the fibers. As a result, the degradation of the MOF that is likely occurring is less obvious because the higher MOF loading still produces a higher surface area than the sample welded for 2 h. In short, these results show that the more the MOF is exposed to the IL, the more likely the MOF will degrade, which will reduce the surface area of the resulting MOF fiber composite.

When the [100 mg, 1 side, 5 h, 0.3 g IL], [100 mg, 1 side, 5 h, 0.6 g IL], and [100 mg, 1 side, 5 h, 0.5 g IL] samples are compared, the results from Table 1 show 2 of the 3 samples produced consistent surface areas of 71 and 76 m^2/g with one sample producing 28 m^2/g. This shows consistent output given the similarity of the preparation of the samples and consistent trends based on the degradation of the MOF in the IL. Specifically, the [100 mg, 1 side, 5 h, 0.3 g IL] sample resulted in a TGA MOF loading of 12 wt % and a surface area of 28 m^2/g, and when the IL was increased to 0.6 g in the [100 mg, 1 side, 5 h, 0.6 g IL] sample, the MOF loading by the TGA increased to 24 wt % and the surface area of the fabric increased to 71 m^2/g. This is consistent with the [100 mg, 1 side, 5 h, 0.5 g IL] sample that shows an 18 wt % MOF loading by the TGA and a 76 m^2/g surface area. The loading of the MOF, as determined by the TGA, is consistent with the increase in the IL used for the welding. The 0.6 g sample shows the highest MOF loading by the TGA, 24 wt %, but the surface area is nearly the same as the sample that used 0.5 g of the IL resulting in a TGA MOF loading of 18 wt %. This is likely occurring because of degradation of the MOF and minor variances of the sample area between similarly prepared samples.

Additional 1 × 1 in. swatches were produced to examine repeatability and the impact of different MOF loading amounts, heating times, and additional washing steps. As shown in Figure 6, the PXRD patterns of three samples are shown with the initial results as the top three PXRD data sets, and the data show that even after washing the samples in water for an additional 24 h, the PXRD pattern is maintained. The presence of a UiO-66-NH_2 PXRD pattern after 48 h of washing is consistent with these samples maintaining a measurable BET surface area.

To inspect the surface of the fibers, SEM images were collected on the fabric samples and are shown in Figure 7. Figure 7b displays [100 mg, 1 side, 5 h, 0.3 g IL] at 500× magnification, which exhibited readily observable differences between the MOF-welded fibers and the control textile. The box shows where voids have been filled after the welding

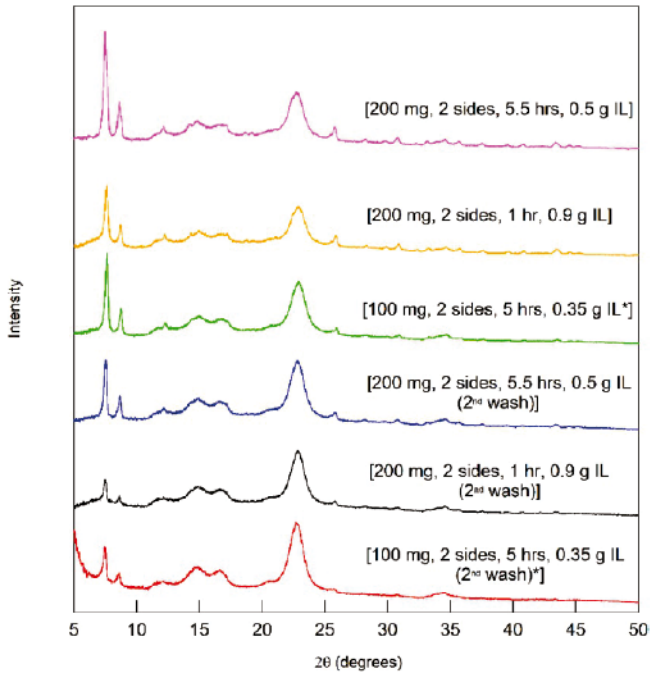

Figure 6. PXRD patterns of samples from initial results and after a second wash.

process. The solid material that is seen filling the pores is likely cellulose with entrained MOF. The material filling the voids between the fibers is not an IL because the IL is removed from the fibers during the washing step.

Figure 7c shows that more of the fibers are welded together in [100 mg, 2 sides, 5 h, 0.7 g IL] compared to the [100 mg, 1 side, 5 h, 0.3 g IL] sample shown in Figure 7b. Figure 7d shows the sample [200 mg, 2 sides, 5 h, 2 g IL], which was welded to the point where the fibers were almost welded into a complete sheet. This sample was very stiff and rigid such that when a small piece was cut from the sample for SEM imaging, some cracking occurred. The cracking was not so extensive that the sample was broken to pieces but rather the sample remained intact and fractures were only observed on the SEM images. Based on the SEM images and PXRD results, it was concluded that the [200 mg, 2 sided, 5 h, 2 g IL] sample was welded too much such that the fiber-like properties of the textile were removed relative to the control swatch. In the case [200 mg, 2 sided, 5 h, 2 g IL], it is possible that this material has a much lower water permeation rate than the other samples, and control of the welding conditions may provide a means of tuning the diffusion properties of these materials. Figure 7e,f shows that the fiber modifications remain in place even after a second washing step.

In addition to examining 1-ethyl-3-methylimidazolium acetate, 1-butyl-3-methylimidazolium chloride (C_4mim Cl) was also examined as a welding solvent, and even though several of the samples analyzed had a PXRD pattern consistent with UiO-66-NH_2 and the fabric had the visual appearance consistent with UiO-66-NH_2, it was found that in general, the results obtained using this IL were inconsistent and difficult to predict. Also, a sample prepared using the C_4mim Cl [100 mg, 2 sided, 5 h, and 0.7 g IL] sample had no measurable surface area even though the fabric was not rigid. Based on this data, this IL was not examined further.

https://dx.doi.org/10.1021/acs.iecr.0c03763
Ind. Eng. Chem. Res. 2020, 59, 19285−19298

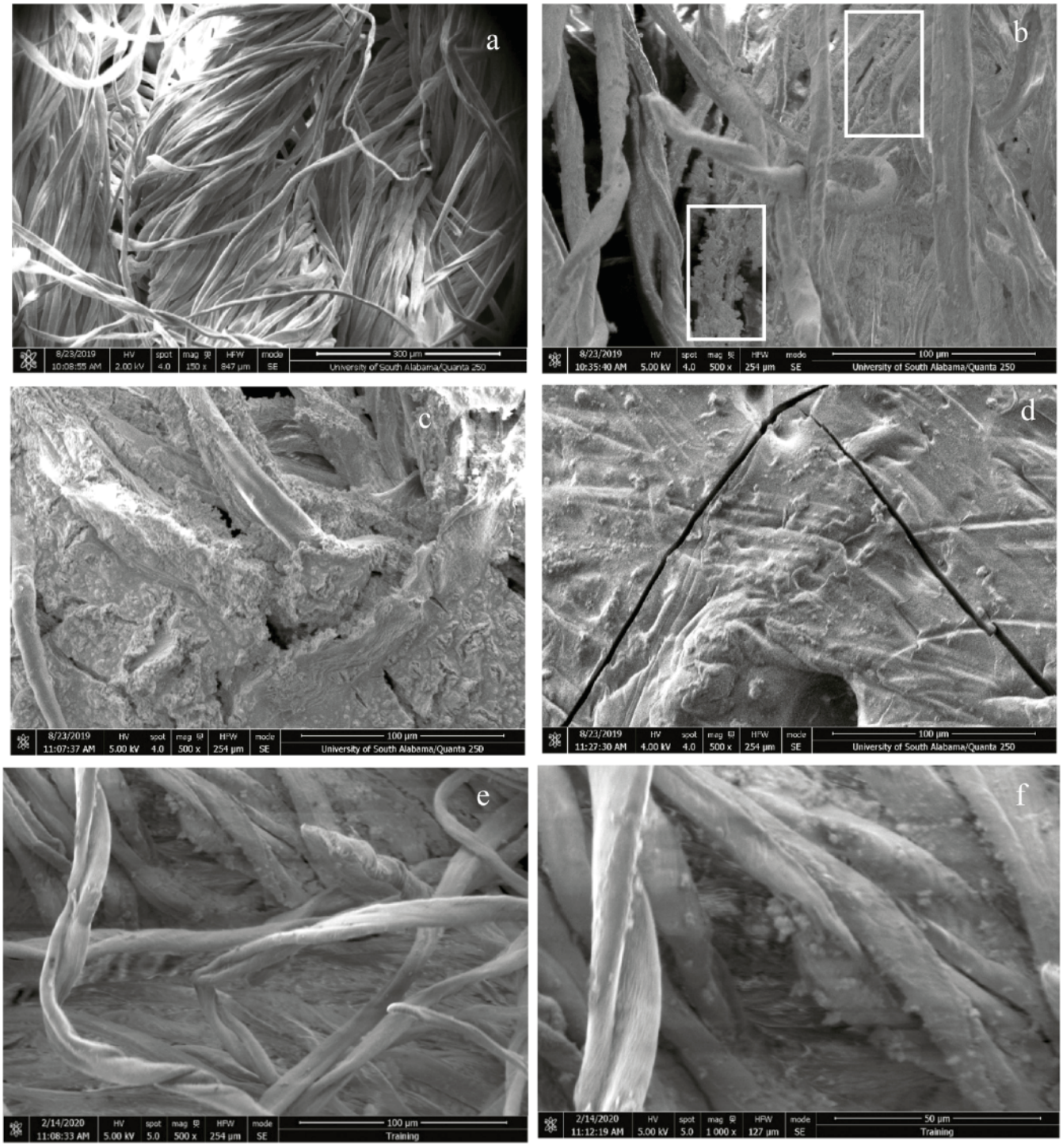

Figure 7. (a) Plain cotton at 150× magnification, (b) [100 mg, 1 side, 5 h, 0.3 g IL] at 500× magnification where the boxes indicate where there are significant changes to the fibers compared to the plain cotton, (c) [100 mg, 2 sides, 5 h, 0.7 g IL] at 500×, (d) [200 mg, 2 sides, 5 h, 2 g IL] at 500× magnification, and (e,f) [200 mg, 2 sides, 5.5 h, 0.5 g IL (second wash)] at 500 and 1000×.

To examine the chemical reactivity of the MOF-modified fabrics, the reaction of DMNP to form *p*-nitrophenoxide in the presence of the fabrics was monitored via UV/Vis by placing the fabric in a buffered solution and allowing the reaction to run over a period of time.[2,3,8,28] During the reaction, aliquots of the reaction solution were removed and analyzed for both DMNP and *p*-nitrophenoxide using UV/VIS spectroscopy. The sample [200 mg, 2 sides, 5.5 h, 0.5 g IL (second wash)] was selected for DMNP analysis and was weighed prior to the DMNP reaction. As a control, pure MOF powder was used in a similar reaction experiment; however, to make an accurate comparison to the fabric, the mass of the MOF on the fabric and the mass of the pure MOF powder used in the control experiment need to be similar, and for this experiment, the wt % MOF on the fabric was determined via the BET surface area method of Bunge et al. The weight was multiplied by the percent MOF on the fabric to obtain the mass of the powder to use in the pure powder control experiment. In this case, the

https://dx.doi.org/10.1021/acs.iecr.0c03763
Ind. Eng. Chem. Res. 2020, 59, 19285−19298

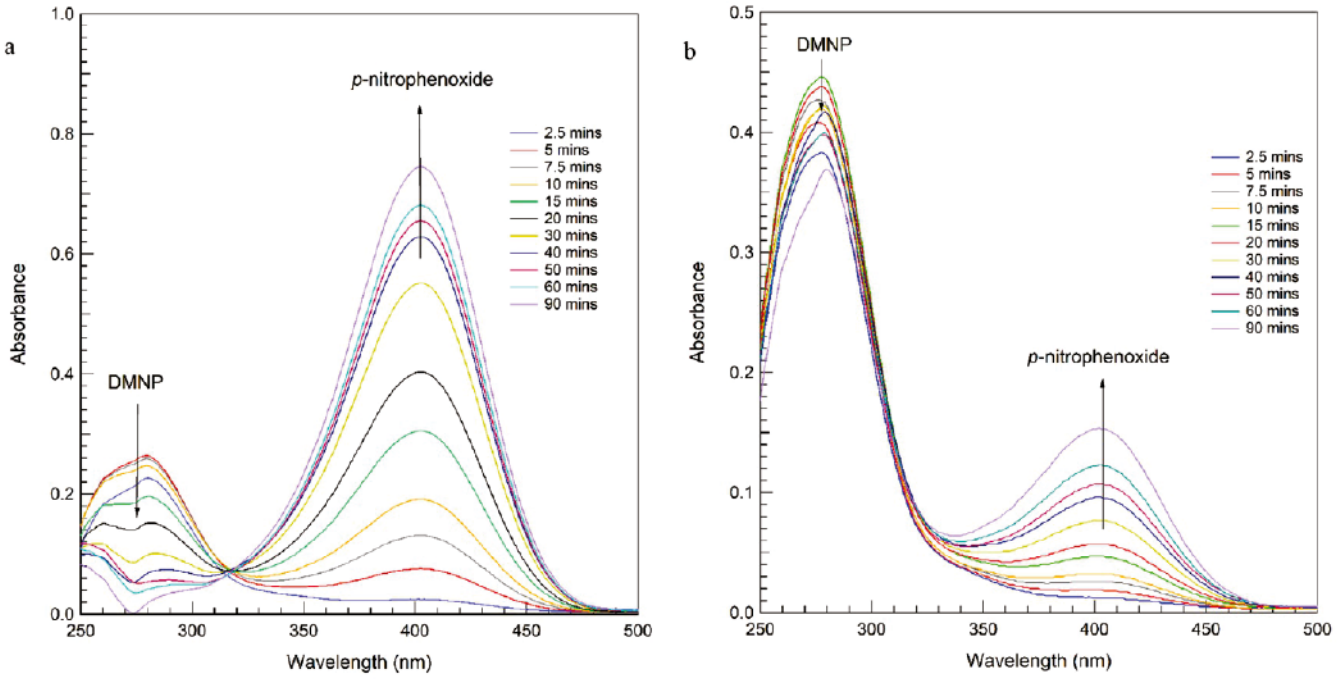

Figure 8. DMNP reactions from sample (a) [200 mg, 2 sides, 5.5 h, 0.5 g IL (second wash)] and (b) UiO-66-NH_2 powder.

weight percent of the MOF on the fabric was calculated based on the pure powder MOF BET loading versus the controls shown in Table 1, as a conservative estimate of MOF loading.

First-order reaction rate kinetics were assumed (spectroscopic data shown in Figure 8) and the half-life was calculated and is shown in Table 2. DMNP reaction experiments on samples, [100 mg, 1 side, 5 h, 0.3 g IL] and [200 mg, 2 sides, 5.5 h, 0.5 g IL (2nd wash)], were completed twice, and both results are presented in the table for comparison. The results show that the fabric sample reacted with DMNP to produce *p*-nitrophenoxide more quickly than the pure powder. The faster reaction time of the fabric versus the pure MOF powder may have occurred because of decreased mass transfer resistances by having the MOF dispersed in the fabric and possibly wicking of DMNP into the cotton fibers. It is also possible that the BET area method has underestimated the amount of MOF on the fabric, which would also influence the kinetic calculations for the pure MOF powder control. Using the TGA method would have also resulted in some error as the TGA method would have likely overestimated the amount of MOF on the fabric. Finally, there are slight differences in half-life, which may be occurring because of variations in the MOF on the fabric swatches.

Table 2. DMNP Half-Life Data

sample	half-life (mins)
plain cotton	330
UiO-66-NH2 powder	41.5
[100 mg, 1 side, 5 h (a), 0.3 g IL]	18
[100 mg, 1 side, 5 h (a), 0.3 g IL run 2]	10
[200 mg, 2 sides, 5.5 h, 0.5 g IL (2nd wash)]	4
[200 mg, 2 sides, 5.5 h, 0.5 g IL (2nd wash)] run 2	6.5

Large-Scale MOF Cotton Swatches. As a control, 5 × 5 in. pieces of fabric were prepared using only the IL. The swatch shown in Figure 9 was prepared by applying 6 g of the IL to both sides of a 4.5 × 3.5 in. fabric. The fabric was pressed between paper towels to remove any excess solution. Shrinking of the fabric swatches was observed with the welded 4.5 × 3.5 in. control fabric being reduced to approximately 3.5 × 2 in.

Next, a 5 × 5 in. UiO-66-NH_2 fabric sample was prepared following the experimental procedure described above but with an IL MOF solution. Figure 9 displays the sample after the welding process, washing, and drying. The unmodified cotton fabric swatch began as a 5 × 5 in. swatch but shrank to approximately 4 × 4 in. after the welding and washing processes. An aluminum block, acting as a heat sink, usually lays on top of the fabric while it is in the oven, however, with the larger swatch, the block was only able to cover part of the sample, which produced an interesting result. In this case, the portions of the fabric that were not under the metal were more rigid than the center part of the fabric. The center and edge were both analyzed with PXRD, and the surface area of the center piece and edge was 22 and 56 m^2/g, respectively. Although the edge had a higher surface area, the texture of the fabric was significantly more rigid on the edge of the fabric than the center. It is possible that the aluminum block used to provide uniform heating is also restraining the fabric and preventing it from contracting during welding. As a result of limiting the movement of the fibers, less MOF material is retained in the weld, resulting in a lower fabric surface area.

Additionally, a large 15.5 × 15.5 in. swatch was prepared via the direct-contact method by welding a piece of cotton, as shown in Figure 10. The final measurement of the fabric after the welding process was approximately 10 × 15 in., where the shrinking is consistent with the 5 × 5 in. samples. A small square was cut off the corner of the welded swatch to characterize the sample. The large direct-contact method swatch had to be washed a second time to ensure that loose MOF dust had been removed from the fabric. PXRD results are consistent with the pure MOF powder, and the BET surface area was 97 m^2/g equivalent to 7.7 wt % MOF loading

https://dx.doi.org/10.1021/acs.iecr.0c03763
Ind. Eng. Chem. Res. 2020, 59, 19285−19298

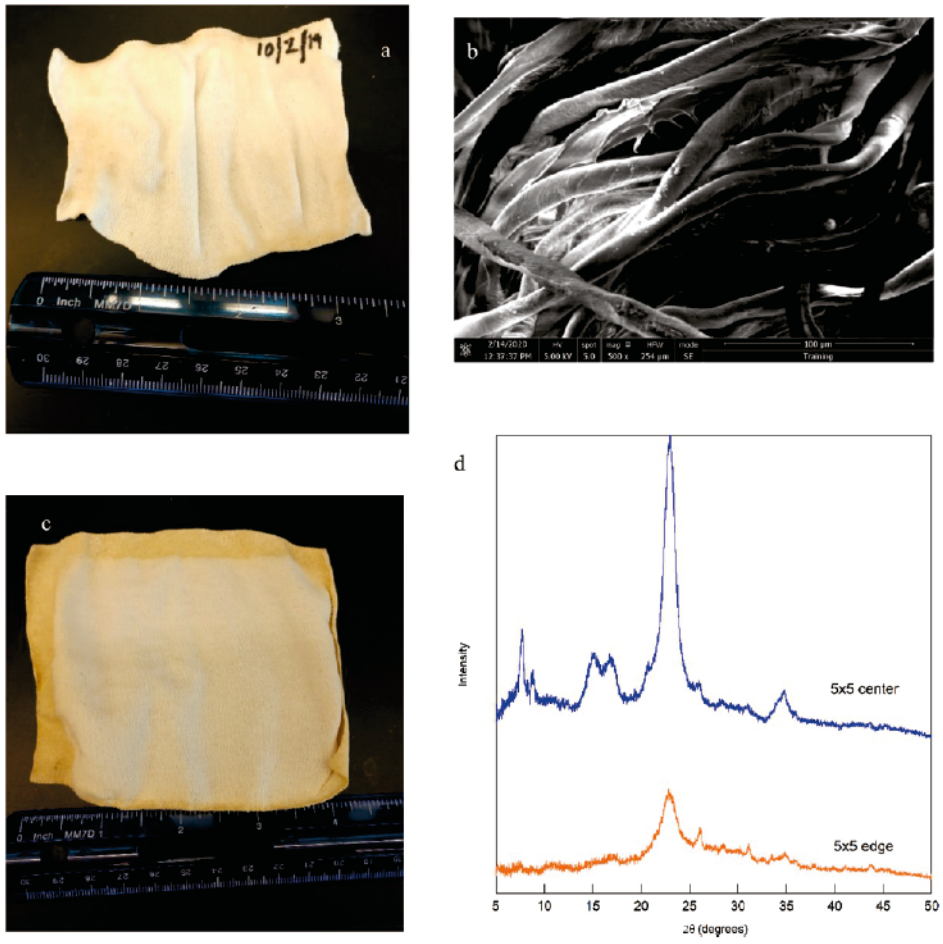

Figure 9. IL applied on larger fabric swatches without the MOF showing the impact of welding conditions on the shrinking of the fabric. (a) 6 g of the IL applied to a 4.5 × 3.5 in. fabric and (b) SEM image of 1 g of the IL applied to a 1.5 × 1.5 in. swatch. The shrinking can be controlled by reducing the amount of IL used for welding or by diluting the IL in a solvent, such as methanol. (c) 5 × 5 in. cotton swatch after the UiO-66-NH_2 welding process and (d) PXRD patterns for the swatch.

Figure 10. (a) Plain cotton 15.5 × 15.5 in., (b) fabric swatch after the UiO-66-NH_2 IL welding process, and (c) PXRD pattern of the swatch shown in (b).

by mass. This result illustrates that it is possible to produce larger-scale MOF textiles using IL welding.

Airbrush-Welding Method. In addition to producing samples with the direct-contact method, samples were also prepared using an airbrush. The IL/UiO-66-NH_2 mixture was added to the airbrush, sprayed onto the swatch, the swatch was subsequently placed in the oven at 80 °C, and then washed after it was removed from the oven. Figure 11a displays the image of an airbrush sample after the welding and washing process. This sample, [Airbrush 1 0.3 g, 2 sides, 2 h, 2.5 g IL], was approximately 2 × 2 in. and had a surface area of 20 m^2/g. Two other samples with more MOF in the IL mixture were prepared, which produced the samples [Airbrush 2 0.4 g, 2 sides, 2 h, 2.1 g IL] that had a surface area of 33 m^2/g and

https://dx.doi.org/10.1021/acs.iecr.0c03763
Ind. Eng. Chem. Res. 2020, 59, 19285−19298

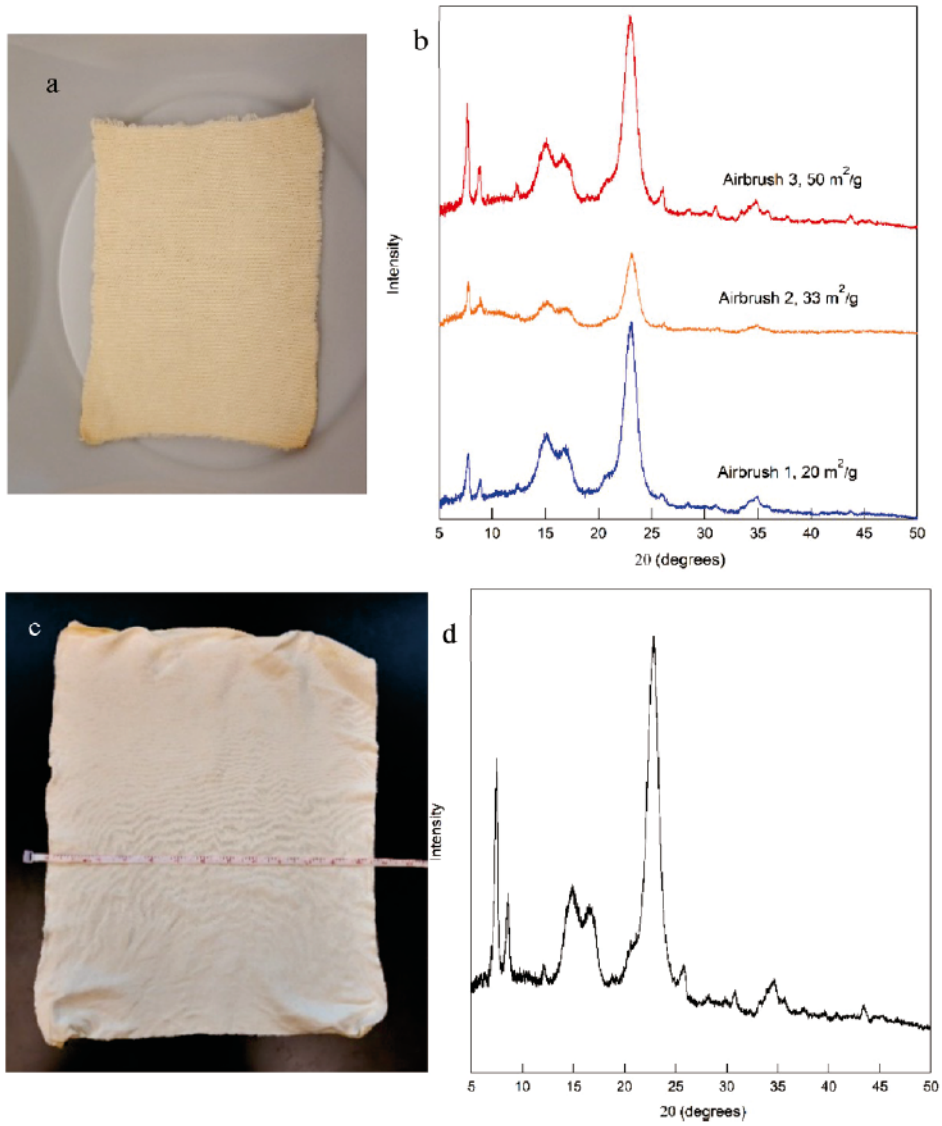

Figure 11. (a) Image of [Airbrush 1 0.3 g, 2 sides, 2 h, 2.5 g IL] that had a surface area of 20 m^2/g and is approximately 2 × 2 in. in size. (b) PXRD patterns of the airbrush samples with their respective surface areas (c) 12.5 × 16 in. UiO-66-NH_2 airbrush swatch and (d) PXRD pattern of the swatch.

[Airbrush 3 0.75 g, 2 sides, 2 h, 4.1 g IL] with a surface area of 50 m^2/g. PXRD patterns of these swatches are shown in Figure 11b, which show peaks consistent with UiO-66-NH_2. The airbrush method provided an even coating of the MOF welding solution on the fibers, and the loading was readily controlled by varying the amount of MOF in the IL.

Additionally, a larger 15 × 16 in. swatch was also produced using the airbrush method, and after welding, the swatch was approximately 12.5 × 16 in., as shown in Figure 11c. Not as much shrinking was observed in the airbrush sample compared to the direct-contact method. The application of the MOF onto the fibers appeared more evenly coated on the airbrush sample when compared to the direct-contact method. This sample was washed once, and the MOF did not come off as a dust. A small piece of fabric was cut from one of the corners to examine PXRD and surface area. PXRD results are displayed in Figure 11d and are consistent with the UiO-66-NH_2 pattern. The surface area for this sample was 56 m^2/g or 4.4 wt % when calculated using the Bunge et al. BET surface area method. SEM images of the large samples prepared using both the airbrush method and the direct contract method are shown in Figure 12.

As was done before, the large samples were tested for their reactivity against the chemical simulant DMNP. Figure 13 displays the spectroscopic data for both large-scale samples. Both samples exhibit a decrease in DMNP and an increase in *p*-nitrophenoxide, which is similar to other UiO-66-NH_2-modified fabric samples. The half-life of the direct-contact method was 2 min, which is faster than the 7 min of the airbrush sample.

MOF-Woven Fabrics. In addition to welding swatches, the welding of individual threads of yarn was examined. In these experiments, CNCs were used to act as a "binder" to help adhere the MOF powder to the cotton yarn and two welding solutions were examined. Both solutions contained a 10 wt % suspension of the MOF by mass in a mixture of EMIm OAc and DMSO and were welded at 80 °C, but one of the solutions had 1.2 wt % CNCs dissolved in the solution and the other did not. It was found that after welding and weaving the yarn, the sample welded with the CNC had a surface area of 22 m^2/g

https://dx.doi.org/10.1021/acs.iecr.0c03763
Ind. Eng. Chem. Res. 2020, 59, 19285−19298

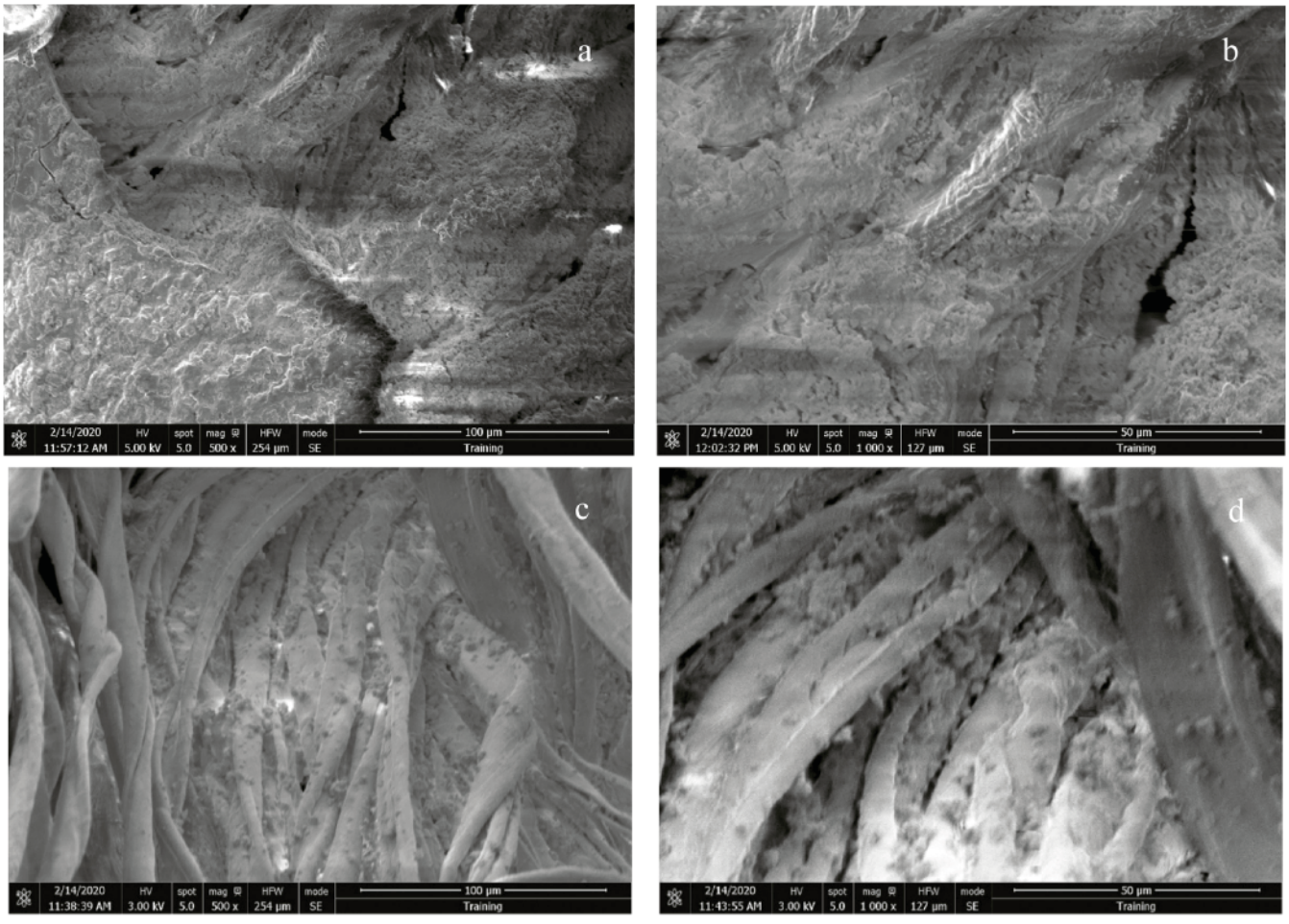

Figure 12. 15.5 × 15.5 in. large swatch prepared using the direct-contact method at (a) 500× and (b) 1000× magnifications. 15 × 16 in. large swatch prepared using the airbrush method at (c) 500× and (d) 1000× magnifications.

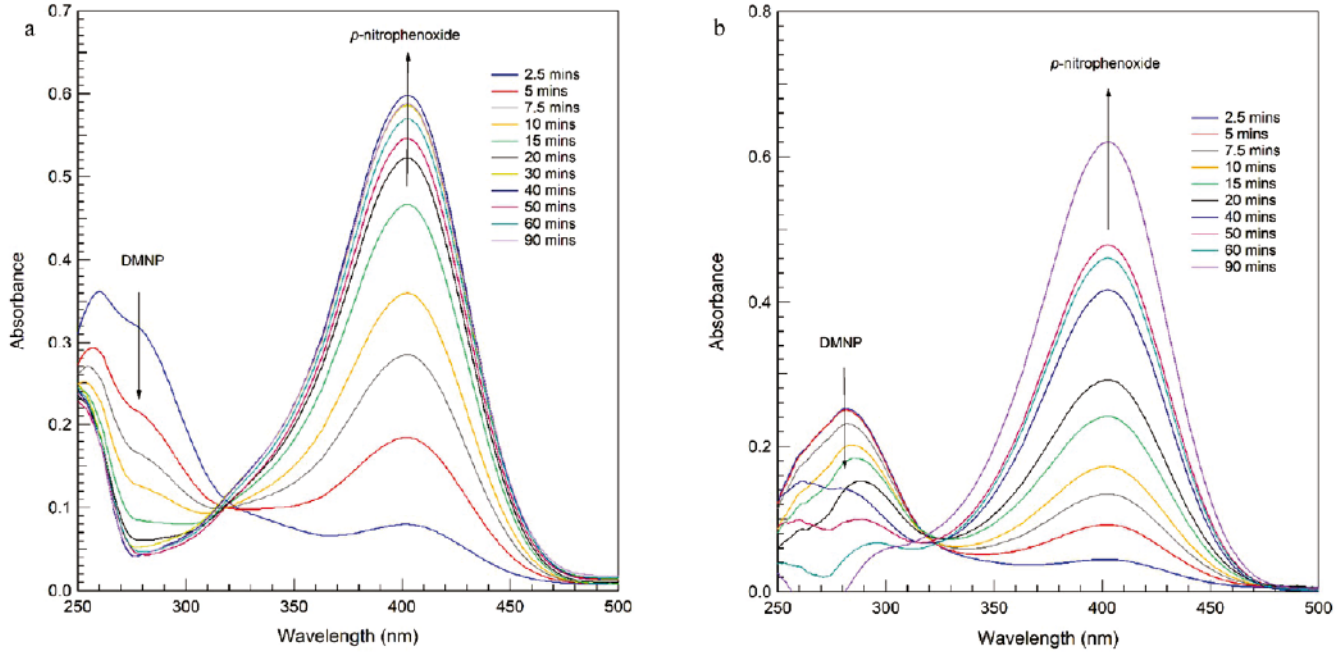

Figure 13. Spectral image of the large samples prepared using the (a) direct-contact method and (b) airbrush method when reacted with DMNP for 90 min. Both observe a decrease in DMNP and an increase in *p*-nitrophenoxide over time.

https://dx.doi.org/10.1021/acs.iecr.0c03763
Ind. Eng. Chem. Res. 2020, 59, 19285−19298

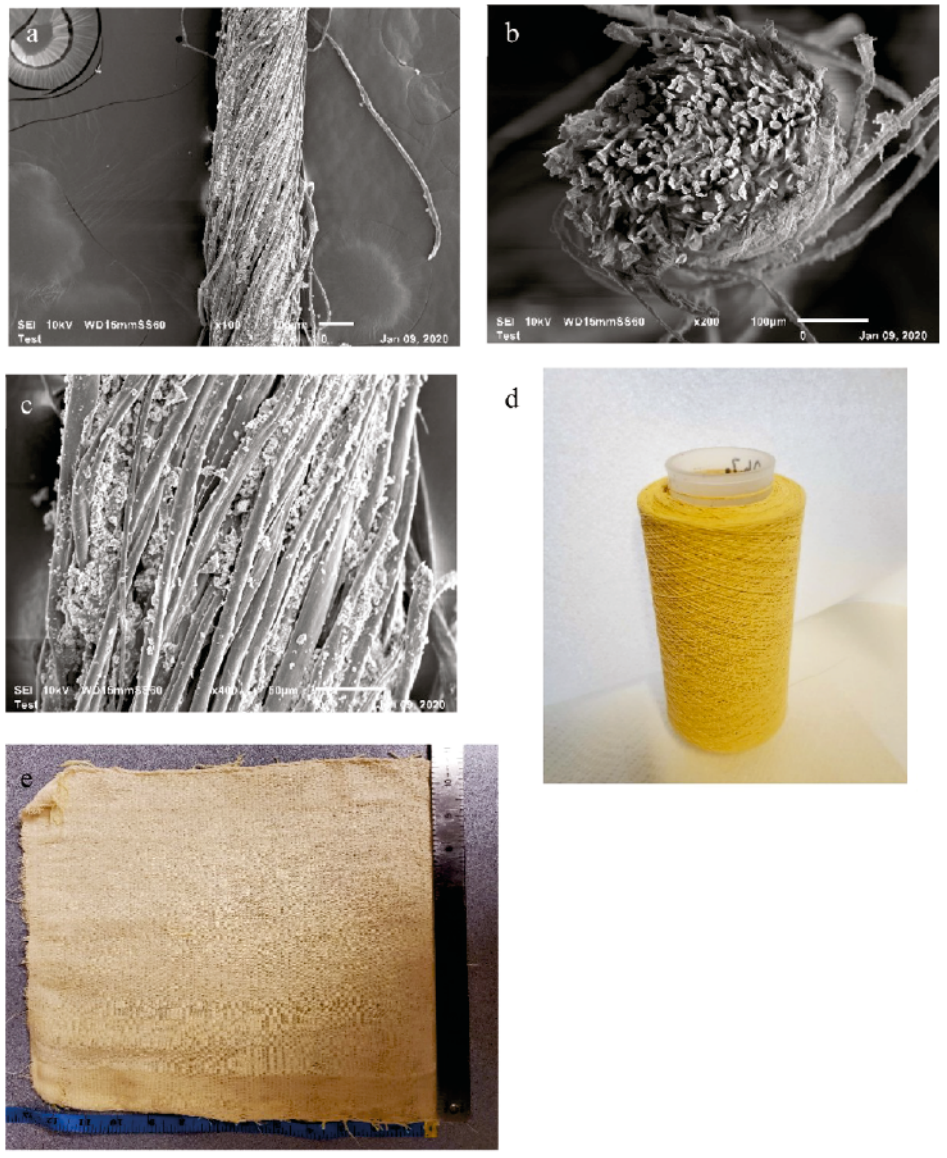

Figure 14. (a,c) Side view and (b) cross-sectional view SEM images of the MOF yarn from the large production run and (d) spool of MOF yarn after production run and (e) 13 × 10.5 in. MOF swatch.

and the one welded without the CNC only had 0.25 m^2/g, indicating that the CNC improves MOF loading when welding strands of yarn.

An IL welding solution of 10 wt % MOF and 1.2 wt % CNCs in a 30/70 mix of EMIm OAc and DMSO welded at 70 °C was selected to produce yarns, as shown in Figure 14. A large spool of yarn was produced (Figure 14d) and the color of the yarn was consistent with the color of the MOF. SEM images of the sample show that the MOF-CNC coating is present on the outside of the yarn while the cross-sectional image shows welding of the cotton yarn, but relative to the control images, it appears that not much MOF is present in the core of the yarn. To demonstrate the ability to weave a fabric with this yarn, a handloom was used to produce a large 13 × 10.5 in. fabric (Figure 14e). Figure 15 displays the PXRD results, showing a pattern consistent with UiO-66-NH_2 on the large 13 × 10.5 in. swatch; however, the surface area of this sample was negligible indicating that the total loading of the MOF on the yarn was low.

■ CONCLUSIONS

The functionalization of cotton textiles with UiO-66-NH_2, ranging in size from 1 × 1 in. to approximately 15 × 15 in., using IL-based fabric welding has been demonstrated. The fabrics show an increase in surface area as a result of MOF loading, PXRD patterns consistent with UiO-66-NH_2, and DMNP reactivity consistent with UiO-66-NH_2. The materials have surface areas that vary from approximately 25 m^2/g to nearly 100 m^2/g depending on the welding conditions used. Three methods were used to produce the fabrics, one where the IL MOF welding solution was directly applied to the fabric, another where the IL MOF welding solution was airbrushed on the fabric, and a third where the MOF was welded to threads and then woven into a textile. Direct application and airbrushing of the MOF IL welding solution to fabrics were able to produce MOF textiles with measurable surface areas and PXRD patterns consistent with UiO-66-NH_2. The application of the MOF IL welding solution to yarn produced a MOF textile with a PXRD pattern consistent with that of UiO-66-NH_2, but the woven textile did not contain any

https://dx.doi.org/10.1021/acs.iecr.0c03763
Ind. Eng. Chem. Res. 2020, 59, 19285−19298

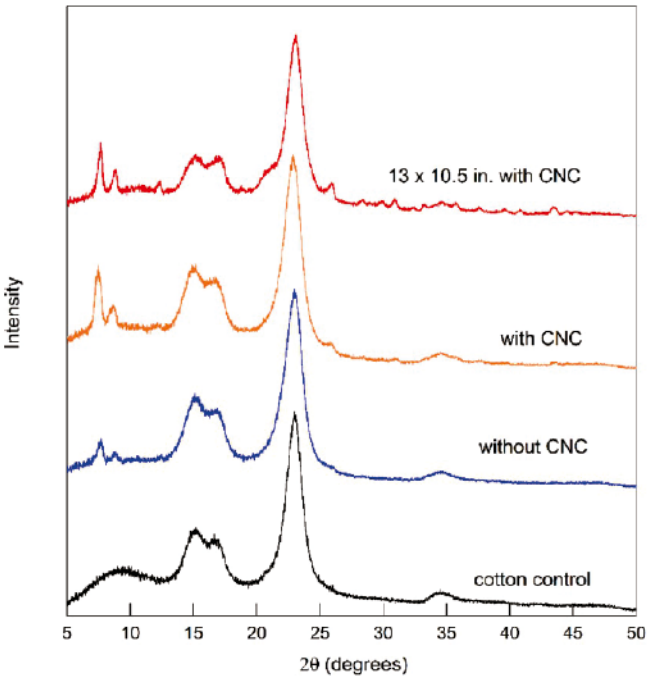

Figure 15. PXRD results of the CNC-welded yarns and swatch woven from MOF-welded yarn.

measurable BET surface area. The results show that IL fiber welding of MOFs is possible and that this method provides a scalable route to attach a variety of MOFs to cotton fabrics.

■ ASSOCIATED CONTENT

Supporting Information

The Supporting Information is available free of charge at https://pubs.acs.org/doi/10.1021/acs.iecr.0c03763.

TGA data of the selected samples (PDF)

■ AUTHOR INFORMATION

Corresponding Author

T. Grant Glover − *University of South Alabama, Mobile, Alabama 36688, United States;* orcid.org/0000-0002-3393-6038; Email: glover@southalabama.edu

Authors

Meagan A. Bunge − *University of South Alabama, Mobile, Alabama 36688, United States;* orcid.org/0000-0002-9286-5030

Erick Pasciak − *Natural Fiber Welding, Inc., Peoria, Illinois 61614, United States*

Jonglak Choi − *Natural Fiber Welding, Inc., Peoria, Illinois 61614, United States*

Luke Haverhals − *Natural Fiber Welding, Inc., Peoria, Illinois 61614, United States*

W. Matthew Reichert − *University of South Alabama, Mobile, Alabama 36688, United States;* orcid.org/0000-0002-8587-2806

Complete contact information is available at: https://pubs.acs.org/10.1021/acs.iecr.0c03763

Notes

The authors declare the following competing financial interest(s): Luke Haverhals is the founder and CEO of Natural Fiber Welding, Inc. that is aiming at commercializing related technologies. Erick Pasciak and Jonglak Choi are employees of Natural Fiber Welding Inc.

■ ACKNOWLEDGMENTS

This work was supported by the United States Army Research Office STTR program under grant no. W911SR19C0014. Imaging that enabled development of materials discussed in this work was supported by the National Science Foundation MRI program under grant no. 1726263. Equipment used in the characterization of the materials was supported by the National Aeronautics and Space Administration Established Program to Stimulate Competitive Research under grant number AL-NNX16AT47A. Any opinions, findings, conclusions, or recommendations expressed in this work are those of the authors and do not necessarily reflect the views of the United States Army, the National Science Foundation, or the National Aeronautics and Space Administration.

■ REFERENCES

(1) Bunge, M. A.; Ruckart, K. N.; Leavesley, S.; Peterson, G. W.; Nguyen, N.; West, K. N.; Glover, T. G. Modification of Fibers with Nanostructures Using Reactive Dye Chemistry. *Ind. Eng. Chem. Res.* **2015**, *54*, 3821−3827.

(2) Bunge, M. A.; Davis, A. B.; West, K. N.; West, C. W.; Glover, T. G. Synthesis and Characterization of UiO-66-NH2 Metal-Organic Framework Cotton Composite Textiles. *Ind. Eng. Chem. Res.* **2018**, *57*, 9151−9161.

(3) Lee, D. T.; Zhao, J.; Peterson, G. W.; Parsons, G. N. Catalytic "MOF-Cloth" Formed via Directed Supramolecular Assembly of UiO-66-NH_2 Crystals on Atomic Layer Deposition-Coated Textiles for Rapid Degradation of Chemical Warfare Agent Simulants. *Chem. Mater.* **2017**, *29*, 4894−4903.

(4) Zhao, J.; Losego, M. D.; Lemaire, P. C.; Williams, P. S.; Gong, B.; Atanasov, S. E.; Blevins, T. M.; Oldham, C. J.; Walls, H. J.; Shepherd, S. D.; Browe, M. A.; Peterson, G. W.; Parsons, G. N. Highly Adsorptive, MOF-Functionalized Nonwoven Fiber Mats for Hazardous Gas Capture Enabled by Atomic Layer Deposition. *Adv. Mater. Interfaces* **2014**, *1*, 1400040.

(5) da Silva Pinto, M.; Sierra-Avila, C. A.; Hinestroza, J. P. In situ synthesis of a Cu-BTC metal-organic framework (MOF 199) onto cellulosic fibrous substrates: cotton. *Cellulose* **2012**, *19*, 1771−1779.

(6) Schelling, M.; Kim, M.; Otal, E.; Hinestroza, J. Decoration of Cotton Fibers with a Water-Stable Metal-Organic Framework (UiO-66) for the Decomposition and Enhanced Adsorption of Micro-pollutants in Water. *Bioengineering* **2018**, *5*, 14.

(7) Ma, K.; Islamoglu, T.; Chen, Z.; Li, P.; Wasson, M. C.; Chen, Y.; Wang, Y.; Peterson, G. W.; Xin, J. H.; Farha, O. K. Scalable and Template-Free Aqueous Synthesis of Zirconium-Based Metal-Organic Framework Coating on Textile Fiber. *J. Am. Chem. Soc.* **2019**, *141*, 15626−15633.

(8) Lu, A. X.; McEntee, M.; Browe, M. A.; Hall, M. G.; DeCoste, J. B.; Peterson, G. W. MOFabric: Electrospun Nanofiber Mats from PVDF/UiO-66-NH2 for Chemical Protection and Decontamination. *ACS Appl. Mater. Interfaces* **2017**, *9*, 13632−13636.

(9) Peterson, G. W.; Lu, A. X.; Epps, T. H. Tuning the Morphology and Activity of Electrospun Polystyrene/UiO-66-NH2 Metal-Organic Framework Composites to Enhance Chemical Warfare Agent Removal. *ACS Appl. Mater. Interfaces* **2017**, *9*, 32248−32254.

(10) *Gas Adsorption in Metal−Organic Frameworks: Fundamentals and Applications*; Glover, T. G., Mu, B., Eds.; Taylor & Francis, 2018.

(11) Flowers, P.; Theopold, K.; Langley, R.; Neth, E. J.; Robinson, W. R. *Chemistry: Atoms First 2e*; OpenStax, 2019.

(12) Marsh, K. N.; Boxall, J. A.; Lichtenthaler, R. Room temperature ionic liquids and their mixtures-a review. *Fluid Phase Equilib.* **2004**, *219*, 93−98.

(13) Bates, E. D.; Mayton, R. D.; Ntai, I.; Davis, J. H. CO2Capture by a Task-Specific Ionic Liquid. *J. Am. Chem. Soc.* **2002**, *124*, 926−927.
(14) Bradaric, C. J.; Downard, A.; Kennedy, C.; Robertson, A. J.; Zhou, Y. Industrial Preparation of Phosphonium Ionic Liquids. *Green Chem.* **2003**, *5*, 143−152.
(15) Dinarès, I.; Garcia de Miguel, C.; Ibáñez, A.; Mesquida, N.; Alcalde, E. Imidazolium Ionic Liquids: A Simple Anion Exchange Protocol. *Green Chem.* **2009**, *11*, 1507.
(16) Alcalde, E.; Dinarès, I.; Ibáñez, A.; Mesquida, N. A general halide-to-anion switch for imidazolium-based ionic liquids and oligocationic systems using anion exchange resins (A− form). *Chem. Commun.* **2011**, *47*, 3266.
(17) Haverhals, L. M.; Reichert, W. M.; De Long, H. C.; Trulove, P. C. Natural Fiber Welding. *Macromol. Mater. Eng.* **2010**, *295*, 425−430.
(18) Haverhals, L. M.; Sulpizio, H. M.; Fayos, Z. A.; Trulove, M. A.; Reichert, W. M.; Foley, M. P.; De Long, H. C.; Trulove, P. C. Process Variables That Control Natural Fiber Welding: Time, Temperature, and Amount of Ionic Liquid. *Cellulose* **2012**, *19*, 13−22.
(19) Durkin, D. P.; Ye, T.; Choi, J.; Livi, K. J. T.; Long, H. C. D.; Trulove, P. C.; Fairbrother, D. H.; Haverhals, L. M.; Shuai, D. Sustainable and Scalable Natural Fiber Welded Palladium-Indium Catalysts for Nitrate Reduction. *Appl. Catal., B* **2018**, *221*, 290−301.
(20) Haverhals, L.; Isaacs, T. A.; Page, E.; Reichert, W. M.; De Long, H. C.; Trulove, P. C. Ionic Liquids in the Preparation of Biopolymer Composite Materials. *ECS Transactions*; ECS: Honolulu, HI, 2009; pp 129−139.
(21) Haverhals, L. M.; Sulpizio, H. M.; Fayos, Z. A.; Trulove, M. A.; Reichert, W. M.; Foley, M. P.; De Long, H. C.; Trulove, P. C. Process Variables That Control Natural Fiber Welding. *ECS Trans.* **2010**, *33*, 79−90.
(22) Haverhals, L. M.; Sulpizio, H. M.; Fayos, Z. A.; Trulove, M. A.; Reichert, W. M.; Foley, M. P.; De Long, H. C.; Trulove, P. C. Characterization of Polymer Movement in Fiber Welded Cellulose Composites. *ECS Trans.* **2010**, *33*, 91−98.
(23) Ruckart, K. N.; O'Brien, R. A.; Woodard, S. M.; West, K. N.; Glover, T. G. Porous Solids Impregnated with Task-Specific Ionic Liquids as Composite Sorbents. *J. Phys. Chem. C* **2015**, *119*, 20681−20697.
(24) Ruckart, K. N.; Zhang, Y.; Reichert, W. M.; Peterson, G. W.; Glover, T. G. Sorption of Ammonia in Mesoporous-Silica Ionic Liquid Composites. *Ind. Eng. Chem. Res.* **2016**, *55*, 12191−12204.
(25) Rudisill, E. N.; Hacskaylo, J. J.; LeVan, M. D. Coadsorption of Hydrocarbons and Water on BPL Activated Carbon. *Ind. Eng. Chem. Res.* **1992**, *31*, 1122−1130.
(26) Luan, Y.; Qi, Y.; Gao, H.; Andriamitantsoa, R. S.; Zheng, N.; Wang, G. A general post-synthetic modification approach of amino-tagged metal-organic frameworks to access efficient catalysts for the Knoevenagel condensation reaction. *J. Mater. Chem. A* **2015**, *3*, 17320−17331.
(27) Rouquerol, J.; Llewellyn, P.; Rouquerol, F. Is the Bet Equation Applicable to Microporous Adsorbents? In *Studies in Surface Science and Catalysis*; Llewellyn, P. L., Rodriquez-Reinoso, F., Rouqerol, J., Seaton, N., Eds.; Characterization of Porous Solids VII; Elsevier, 2007; Vol. *160*, pp 49−56.
(28) Mondloch, J. E.; Katz, M. J.; Isley, W. C., III; Ghosh, P.; Liao, P.; Bury, W.; Wagner, G. W.; Hall, M. G.; DeCoste, J. B.; Peterson, G. W.; Snurr, R. Q.; Cramer, C. J.; Hupp, J. T.; Farha, O. K. Destruction of chemical warfare agents using metal-organic frameworks. *Nat. Mater.* **2015**, *14*, 512−516.

https://dx.doi.org/10.1021/acs.iecr.0c03763
Ind. Eng. Chem. Res. 2020, 59, 19285−19298